

Experimental Demonstration of Extended 5G Digital Fronthaul over a Partially-Disaggregated WDM/SDM Network

Citation for published version (APA):

Fabrega, J. M., Munoz, R., Nadal, L., Manso, C., Svaluto Moreolo, M., Vilalta, R., Martinez, R., Vilchez, F. J., Perez Galacho, D., Sales, S., Grivas, E., Turkiewicz, J. P., Rommel, S., & Tafur Monroy, I. (2021). Experimental Demonstration of Extended 5G Digital Fronthaul over a Partially-Disaggregated WDM/SDM Network. *IEEE Journal on Selected Areas in Communications*, 39(9), 2804-2815. Article 9373342. Advance online publication. <https://doi.org/10.1109/JSAC.2021.3064645>

DOI:

[10.1109/JSAC.2021.3064645](https://doi.org/10.1109/JSAC.2021.3064645)

Document status and date:

Published: 01/09/2021

Document Version:

Accepted manuscript including changes made at the peer-review stage

Please check the document version of this publication:

- A submitted manuscript is the version of the article upon submission and before peer-review. There can be important differences between the submitted version and the official published version of record. People interested in the research are advised to contact the author for the final version of the publication, or visit the DOI to the publisher's website.
- The final author version and the galley proof are versions of the publication after peer review.
- The final published version features the final layout of the paper including the volume, issue and page numbers.

[Link to publication](#)

General rights

Copyright and moral rights for the publications made accessible in the public portal are retained by the authors and/or other copyright owners and it is a condition of accessing publications that users recognise and abide by the legal requirements associated with these rights.

- Users may download and print one copy of any publication from the public portal for the purpose of private study or research.
- You may not further distribute the material or use it for any profit-making activity or commercial gain
- You may freely distribute the URL identifying the publication in the public portal.

If the publication is distributed under the terms of Article 25fa of the Dutch Copyright Act, indicated by the "Taverne" license above, please follow below link for the End User Agreement:

www.tue.nl/taverne

Take down policy

If you believe that this document breaches copyright please contact us at:

openaccess@tue.nl

providing details and we will investigate your claim.

Experimental Demonstration of Extended 5G Digital Fronthaul over a Partially-Disaggregated WDM/SDM Network

J. M. Fabrega, *Senior Member, IEEE*, R. Muñoz, *Senior Member, IEEE*, L. Nadal, *Senior Member, IEEE*, C. Manso, M. Svaluto Moreolo, *Senior Member, IEEE*, R. Vilalta, *Senior Member, IEEE*, R. Martínez, *Senior Member, IEEE*, F. J. Vílchez, *Senior Member, IEEE*, D. Pérez Galacho, S. Sales, *Senior Member, IEEE*, E. Grivas, J. P. Turkiewicz, S. Rommel, and I. Tafur Monroy

Abstract—We experimentally demonstrate a 5G digital fronthaul network that relies on multi-adaptive bandwidth/variable transceivers (BVTs) and an autonomic software-defined networking (SDN) control system for partially-disaggregated wavelength division multiplexing (WDM)/space division multiplexing (SDM). Transmission of 256-QAM 760.32 MHz orthogonal frequency-division multiplexing (OFDM) radio signal is performed, with a total radio transmission capacity of 5.667 Gb/s. Digitized signal samples are carried as a 22.25 Gb/s digitized radio-over-fiber (DRoF) data stream and transmitted over a WDM/SDM infrastructure including 40-wavelength 100-GHz arrayed waveguide gratings (AWGs) and 19-core fiber. The autonomic SDN controller deploys a control loop for the multi-adaptive OFDM-based BVTs that monitors the per-subcarrier signal to noise ratio (SNR) and assigns the optimal constellation based on the actual signal degradation. An error vector magnitude (EVM) below the targeted 2.1% is achieved while setting up connections in less than 5 s.

Index Terms—Fronthaul, Optical Networks, Optical transmission, SDM, 5G, SDN.

I. INTRODUCTION

THE DRoF is a popular fronthaul technology that is being deployed worldwide for giving service to radio access networks (RANs) [1]. This allows centralization with clear advantages in the reduction of costs in the external plant, as remote radio units (RRUs) are expected to have a smaller installation footprint and energy consumption than a classic base station [1]. With the increasing capacity demand of 5G,

Work supported by the EC H2020 BLUESPACE (762055) and Spanish MICINN AURORAS (RTI2018-099178) projects.

J. M. Fabrega, R. Muñoz, L. Nadal, C. Manso, M. Svaluto Moreolo, R. Vilalta, R. Martínez and F. J. Vílchez are with the Optical Networks and Systems Department of the Centre Tecnològic de Telecomunicacions de Catalunya (CTTC/CERCA), Castelldefels, Spain, e-mail: jm-fabrega@cttc.es, rmunoz@cttc.es, lnadal@cttc.es, cmanso@cttc.es, msvaluto@cttc.es, rvilalta@cttc.es, rmartinez@cttc.es, jvilchez@cttc.es

D. Pérez Galacho and S. Sales are with the ITEAM institute, Universitat Politècnica de València, Valencia, Spain, e-mail: diepega@iteam.upv.es, ssaes@iteam.upv.es

E. Grivas is with Eulambia Advanced Technologies Ltd., Athens, Greece, e-mail: egrivas@eulambia.com

J. P. Turkiewicz is with Orange Polska, Warsaw, Poland; and also with Warsaw University of Technology, Warsaw, Poland; e-mail: Jaroslaw.Turkiewicz@orange.com

S. Rommel and I. Tafur Monroy are with the Institute for Photonic Integration, Eindhoven University of Technology, Eindhoven, Netherlands, e-mail: s.rommel@tue.nl, i.tafur.monroy@tue.nl

Manuscript received July 15th, 2020; revised YYYY; published ZZZZ.

new radio (5G-NR) waveforms and processing are expected in an environment where small cells are massively deployed at high density [1], [2]. In fact, [2] specifies new radio waveforms featuring increased bandwidth and constellation size, able to cope with capacities beyond 1 Gb/s per user. Since bandwidth and constellation size are increased, DRoF fronthaul requires a significantly large capacity even for transmitting a single radio signal.

This puts DRoF technology at stake, requiring further evolution to keep scaling up while meeting its latency requirements. This need can be addressed by adapting DRoF to cope with an upgraded fiber plant that includes SDM by deploying multi-core fibers (MCFs) [3], [4]. Current estimations for DRoF show that several hundreds of Gb/s, and even Tb/s will be needed per antenna site in the upcoming years [5]. Therefore, the use of MCFs is the straightforward solution to cope with these needs in a cost effective way [6]. By combining WDM and SDM, the total capacity of a RAN can be substantially increased, enabling to setup specific WDM/SDM channels according to the requirements of the services to deliver [7]. In this sense, the so-called BVTs constitute a key element for optical fronthaul transmission [8], [9]. The BVTs implement a range of advanced functionalities, such as a dynamic variation and adaptation of modulation format and symbol rate. In this regards, optical OFDM is a promising candidate thanks to its superior granularity and capabilities for transmission re-configuration [10]. OFDM allows adaptive modulation format selection at subcarrier level according to the channel profile.

In terms of network development, the telecom operators are looking at the optical network disaggregation approach because it entails cost-reduction while enabling the migration and upgrade of network components and avoiding vendor lock-in [11]. In fact, two optical disaggregation models can be considered: partially or fully disaggregated. In the first model, multiple vendors provide the transponders with open application programming interfaces (APIs) to interface with the transport SDN controller; whilst the remaining elements, known as the optical line system (OLS), remain as a single-vendor infrastructure [11]. A different vendor provides the OLS controller with open APIs to interface with the transport SDN controller. In the second model, different vendors provide all the optical network elements, each featuring a standard APIs (e.g. OpenConfig or OpenROADM) to the transport SDN

controller. Each of these elements has a unified data model and open APIs to the SDN control system.

In this paper, we experimentally demonstrate a DRoF approach based on optical OFDM that uses WDM/SDM in combination with an agile data plane and advanced control plane. Our approach also aims at integrating the optical access and metro networks, both at the transport and control level, thanks to the deployed SDM/WDM and using a partially disaggregated infrastructure. So, the same central office (CO) can be shared by different optical access networks that are connected through an optical metro network.

The paper is structured as follows. Section II provides a state of the art in order to contextualize the investigations reported in this paper. In Section III the proposed network scenario is detailed and discussed, providing the details of the data plane and the SDN control system. Section IV, deals with the experimental setup, whereas section V reports the results. Finally, conclusions are drawn in Section VI.

II. PRIOR ART

In traditional RANs, the signal processing of the base-band unit is performed in the base station, together with the RRUs. The transport network supporting the interface between the baseband units (BBUs) and the mobile core (i.e., EPC) is known as mobile backhaul. It has low requirements for delay and bandwidth, and traditionally is deployed in packet-based network infrastructures (e.g. Ethernet, IP/MPLS). The current trend in mobile networks is to evolve towards a centralized radio access network (C-RAN) architecture. In C-RAN, the signal processing of the BBU is decoupled from the RRU and moved far away in the CO [12]. The transport network supporting the communication between the RRUs and the BBUs is known as mobile fronthaul. The key benefits of the C-RAN approach are the cost reduction due to the infrastructure scale effects as well as sophisticated signal processing and control functions [1].

BBU-RRU communication can be either analog or digital. The most simple approach is the analog radio-over-fiber (ARoF), where the analog radio signal generated by the BBUs is directly converted to the optical domain and transmitted over the fiber network. On the contrary, in DRoF the radio signal is digitally sampled and those samples are then transmitted over the fiber network. So, DRoF is very stringent in terms of high-bandwidth and low-delay, since it transports the digitally sampled radio waveform from the RRU to the CO, where the signal processing of the base-band unit is performed [13]. When comparing the performance of deploying DRoF and ARoF over a passive network, the first outperforms the latter in terms of radio signal performance [14].

The most widely used standard interface for the 4G mobile fronthaul is the common public radio interface (CPRI). For 5G, 3GPP is proposing to reduce the bandwidth and latency requirements by moving the signal process of the low PHY back to the base station. In general, 3GPP considers a function split of the baseband processing into eight options [15] that are grouped into three logical entities; the remote unit (RU), the distribution unit (DU), and the central unit (CU). This

brings the introduction of the next generation fronthaul interface (NGFI) that is split into two network segments: NGFI-I between the RU and DU, and the NGFI-II between the DU and CU. 3GPP has already chosen the split option 2 (i.e. split between PDCP and RLC) for NGFI-II, but the splitting between DU and RU is still open. In this sense, there are some studies proposing a flexible and dynamic functional split between the RU and the DU [16].

The mobile fronthaul can be deployed using different transport technologies [17]. For example, a solution that is widely adopted is to deploy point-to-point C/DWDM links with dedicated fiber systems interconnecting the CO with the base station. Another approach is to relay on optical access technologies such as NG-PON2, WDM-P2P, XGS-PON [18]. All these existing fronthaul solutions are in general quite static, meaning that little flexibility and no dynamic reconfiguration can be attained. All these solutions operate on fixed wavelengths (one or more) and at fixed bitrates, offering limited bandwidth. An alternative approach for the NGFI is to deploy packet-based solutions [19]. This, theoretically, enables the use of use of statistical packet multiplexing. However, the packet-based NGFI will introduce new requirements in terms of jitter and synchronization that have to be properly addressed.

Even simple transmission techniques can be used for DRoF (e.g. employing 4PAM modulation with 10G-ready devices) a solution based on BVTs is preferred because of its intrinsic flexibility provided by the numerous parameters that can be configured. In [4] we compared both technologies while setting a trade-off between simplicity against flexibility. In fact, one of the most important features of BVTs is their ability to vary the capacity, which can be programmed by the control plane according to the network requirements [4].

In [20], we proposed for the first time to use a WDM optical networking solution combining SDM, where high capacity and dynamic metro networks with BVTs are installed for realizing a low-cost access network for the mobile fronthaul. SDM is the key technology to overcome the capacity crunch driven by 5G mobile communications in the fronthaul. The simplest way to make use of the spatial dimension is to deploy bundles of single mode fibers, but the final target is exploiting the spatial dimension of the optical fiber having parallel propagation in the same fiber using MCFs. The combination of SDM with WDM enables to exploit the spectral and spatial dimensions in the fronthaul segment and to provide spectral-spatial super-channels [7].

In this paper we extend the architecture presented in [21] by expanding the mobile fronthaul beyond the optical access network. This approach aims at integrating the optical access and metro networks, both at the transport and control level, thanks to the deployed SDM/WDM optical networking solutions. With this approach, it is not needed to deploy a CO at the edge of each optical access network, and the same CO can be share by different optical access networks that are connected through an optical metro network. In this scenario, the latency induced in the mobile fronthaul is very important since it depends on the round-trip time between the RRU and the BBU, that is usually restricted to be lower than 20 ms [22].

The fiber length between BBU and RRU is subject to the optical transmission technology being employed.

Moreover, in this paper we also extend the autonomic SDN control architecture proposed in [23] for partially-disaggregated optical networks, since it can be regarded as the first step when moving towards a fully disaggregated network [11]. To this end, the configuration and monitoring of the integrated access/metro optical network acting as the mobile fronthaul is delegated to a dedicated OLS controller. Then, the SDN controller interfaces with the OLS controller and the BVT agents in order to provide end-to-end fronthaul transport services involving both the access/metro optical network and the BVTs.

Finally, this paper makes use of high-capacity BVT prototypes based on optical OFDM [4], where the corresponding API has been developed to interface with the control plane, allowing a precise control of multiple different transmission parameters.

To the best of our knowledge, this is the first paper addressing partial disaggregation for SDM/WDM optical networking solutions.

The target SDM/WDM fronthaul scenario aims at providing autonomic control of spectral and spatial super-channels with rate/distance adaptive flows. Even a pure fronthaul is targeted in this paper, the solution proposed can be used also in a midhaul scheme, as it relies on the use of BVTs, which can be programmed to fit any capacity [4], [24].

III. CONCEPT AND SCENARIO

The considered disaggregated SDM/WDM fronthaul network with OFDM-based BVTs is shown in Fig. 1. Data and control plane aspects of the network are detailed in the following subsections.

A. Network architecture and systems

The network is composed of COs interconnected through an optical aggregation/metro network deployed with, for example, reconfigurable add-drop multiplexers (ROADMs). The COs serve different cell sites (CSs) through an optical distribution network. At the CO, an optical switch provides connectivity between the ROADMs and the corresponding packet switch that interfaces with a pool of BBUs attached to an array of OFDM-based BVTs [21]. It is worth to mention that not all COs are required to be equipped with a pool of BBUs and BVTs, as shown in Fig. 1. On the access side, the optical switch provides connectivity to either the fan-in/out for SDM transmission [25] or to one or eventually a pool of AWGs or wavelength selective switches (WSSs) for WDM transmission. The CO delivers its data signals to an optical distribution network, whose feeder stage is a MCF that connects the CO with a remote node (RN). At the RN, signals are spatially demultiplexed by means of another fan-in/out device. After the RN, different drop stages are envisioned, either featuring 1-core standard single-mode fiber (SSMF) bundles for continuing SDM scheme or just an SSMF with WDM stages. Finally, the CSs also contain BVTs connected to the RRU and eventual wavelength demultiplexing stages. The RNs are

TABLE I
EXTENDED 5G-NR RADIO PARAMETERS FOR BBU/RRU.

Parameter	Value
Subcarrier spacing	240 kHz
Num. of points for FFT	4096
Sampling frequency (fs)	983.04 MHz
Number of subcarriers	3168
Constellation	16QAM, 64QAM, 256QAM

intended as a main space division demultiplexing point and to eventually serve a macro-cell. The CSs are proposed for a small cell service, using SSMF or a bundle of them for the last mile fronthaul. Please note that MCFs may show certain core-to-core crosstalk with the corresponding impact on the signal performance. So, we need a control system that is able to react to such signal degradation by interacting with the BVTs.

The BVTs are programmable transceivers with enhanced capabilities. In our case, we consider OFDM-based BVTs that feature a broad range of parameters to be configured: maximum and minimum capacity (5-50 Gb/s); modulation (OFDM); number of subcarriers (512); bit per symbol / modulation order (BPSK, 4QAM, 8QAM, 16QAM, 32QAM, 64QAM, 128QAM, 256QAM); nominal central frequency range (191.494 THz - 195.256 THz); bandwidth (25 GHz); forward error correction (FEC) (hard-decision or soft-decision); and equalization (zero-forcing or minimum mean square error (MMSE)). The parameters able to be configured at the BVT are: status (active, off, standby), frequency slot (nominal central frequency and frequency slot width), FEC, equalization, and constellation. Constellation is set in a per subcarrier basis by including two magnitudes: the bits per symbol and the normalized power per symbol. Therefore, the capacity can be flexibly set by the SDN controller by using bit and power loading [26] to configure a suitable constellation. Also, the BVT has a couple of monitored parameters: the overall bit error ratio (BER) giving a general view of the connection performance; and the SNR per subcarrier, in order to have an idea of the channel response for driving the adaptive modulation of the OFDM subcarriers.

Other important elements are the digital BBUs and RRUs, whose schemes are depicted in Fig. 2. The BBUs are composed of a radio signal generation stage, where a digital radio signal is generated according to the parameters listed in Table I. Even though 5G-NR specifies signals up to 400 MHz, in our case we consider an extension to double the standardized bandwidths by combining the maximum subcarrier spacing and maximum number of subcarriers. This signal is then sampled at 983.04 MHz and digitized at M bits per sample, with M ranging between 4 and 20. Please note that the radio signal is clipped at ± 3 times its standard deviation in order to ensure a normalized and unbiased digitization scale. The resulting in-phase and quadrature (I/Q) samples are mapped and framed following the CPRI principles [27]. A 344-bit word is included every 5120 words for control and monitoring purposes. The resulting data is then injected into the corresponding BVT. At the RRU, incoming data from the BVT is deframed, I/Q samples are demapped and the radio signal is reconstructed.

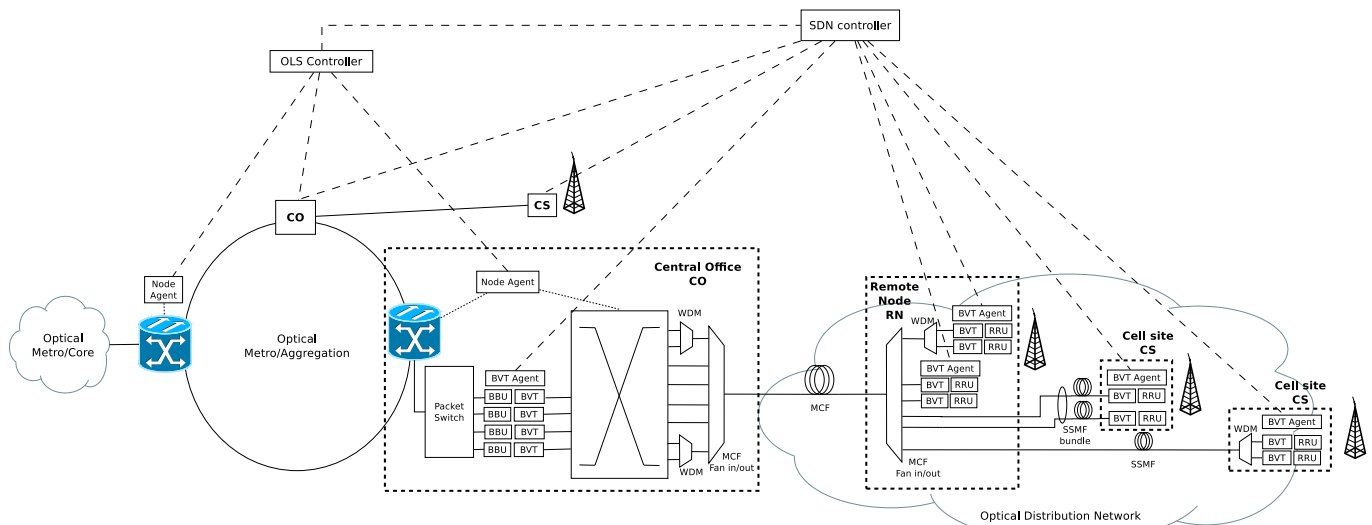


Fig. 1. Example of SDN-controlled partially disaggregated SDM/WDM fronthaul network.

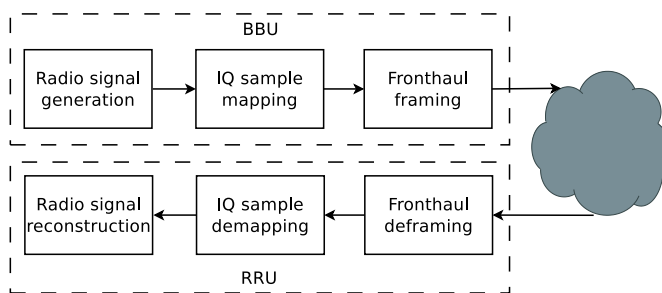


Fig. 2. Internal scheme of BBU and RRU.

The blocks of Fig. 2 have been implemented as a library in Python. A preliminary evaluation is performed in order to evaluate its performance limits and relationship between the figures of merit of DRoF and ARoF. Therefore, an ideal additive white Gaussian noise channel is considered between BBU and RRU blocks. 256 OFDM radio frames are generated and processed accordingly. The control and monitoring words are simple random bits generated for taking into account the associated overhead. BER has been computed by error counting at the input of RRU, while EVM has been computed after radio signal detection. Different radio signal constellations have been tested according to Table I. Results are shown in Fig. 3. There we observe an EVM floor due to signal clipping and the inherent quantization associated to the signal digitization. This EVM floor decreases rapidly when increasing the number of bits per sample (M), converging to values around 0.1 % for all the constellations tested. So $M \geq 10$ can be set as the limit to ensure these values.

Regarding target EVM values before the radio wave radiation elements (after power amplifiers), they are of 12.5 % for 16QAM, 8 % for 64QAM and 3.5 % for 256QAM [2]. Since power amplifiers have typical noise figures of 4.5 dB, the targeted EVM at the output of RRU block is expected to be 7.5 % for 16QAM, 4.8 % for 64QAM and 2.1 % for 256QAM. Therefore, in terms of EVM floor limit, the system

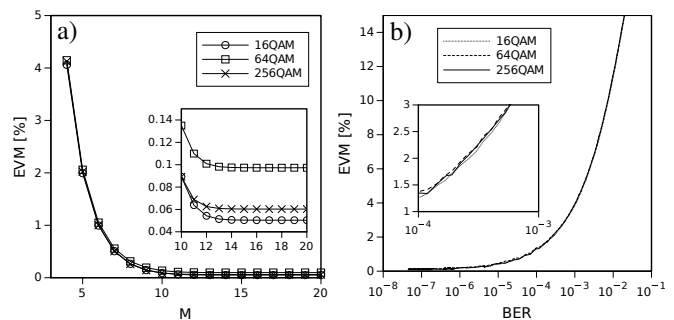


Fig. 3. (a) EVM-floor as a function of the number of bits considered for digitizing. (b) EVM as a function of BER of digitized samples. Insets show zoom to specific areas of the plots.

is compliant with those values for 16QAM and 64QAM, while 256QAM is limited to operate with values of $M > 5$. Please note that 256QAM is the highest order constellation specified in [2]. In terms of BER for the 256QAM case (the most restrictive), we should ensure BER below $2.63 \cdot 10^{-4}$ when considering $M \geq 10$.

B. Autonomic SDN control of OFDM-based BVTs in partially disaggregated SDM/WDM fronthaul networks

The considered SDN control system architecture relies on an optical SDN controller managing a fronthaul OLS controller as well as the multi-adaptive OFDM-based BVTs through dedicated SDN agents, as depicted in Fig.1. Therefore, we are facing a partially disaggregated network, since the SDN controller interacts with the different BVT agents and an OLS controller that takes care of the remaining network infrastructure. In [28] we presented an SDN control system architecture for fully disaggregated networks, where the SDN controller was responsible for configuring all network elements.

The purpose of the BVT agents is to provide a common API to the SDN controller for the configuration and monitoring of the adaptive optical flows. The SDN agent's API defined

for the multi-adaptive OFDM-based BVTs is based on yet another next generation (YANG)/network configuration protocol (NETCONF). We have developed a YANG data model for the configuration functionalities (blueSPACE-DRoF-configuration.yang) and another for the supported capabilities (blueSPACE-DRoF-capability.yang). The BVT YANG models are published online on a public repository at [29]. The parameters that define the supported capabilities by the BVT are: maximum and minimum capacity (5-50 Gb/s), modulation (OFDM), number of subcarriers (512), constellations (BPSK, 4QAM, 8QAM, 16QAM, 32QAM, 64QAM, 128QAM, 256QAM), nominal central frequency range (191.494 THz - 195.256 THz), bandwidth (25 GHz), FEC (hard-decision or soft-decision), and equalization (zero-forcing or minimum mean square error). The parameters able to be configured at the BVT are: status (active, off, standby), frequency slot (nominal central frequency and frequency slot width), FEC, equalization, and constellation. Constellation is set in a per subcarrier basis by means of two vectors: one containing the bits per symbol (e.g. from $L = 2$ up to $L = 8$, corresponding to 2^L quadrature amplitude modulation (QAM)), and another one with the normalized power per symbol for each subcarrier. Therefore, the capacity can be set by the SDN controller by generating the suitable constellation. Also, the BVT has a couple of monitored parameters; the overall BER giving a general view of the connection performance, and the SNR per subcarrier, in order to have an idea of the channel response for driving the adaptive modulation of the OFDM subcarriers. The SDN controller can configure and modify the BVT agents with the allocated nominal central frequency slot, constellation, equalization and FEC by sending NETCONF RPC `<edit-config>` (create/merge). The SDN controller can request the capability parameters or the monitoring parameters by sending NETCONF RPC `<get>` messages to the BVT agents.

The OLS controller manages all switching elements and is responsible for providing transport connectivity services between pairs of BVTs across the whole fronthaul network. A detailed description of the considered fronthaul OLS controller architecture for the target SDM/WDM network with open interfaces is provided in [30] by the authors. The interface between the SDN controller and the fronthaul OLS controller is based on the transport application programming interface (TAPI) [31]. TAPI defines a common YANG data model for the SDN control plane functions (e.g., path computation, topology and connection provisioning) and uses RESTconf as protocol. The optical SDN controller gets a TAPI context from the fronthaul OLS controller. It is defined by a set of service interface points (SIPs), which enables the optical SDN controller to request connectivity services (e.g. optical channels) between any pair of SIPs. Each SIP defines an endpoint available for connections and its characteristics. Similarly, the optical SDN controller also exposes a TAPI context to its customers, e.g a network function virtualization (NFV) orchestrator.

The considered optical SDN controller architecture is depicted in Fig. 4. It is composed of the following modules:

- Service orchestrator: Processes the incoming TAPI requests from the northbound interface and handles the

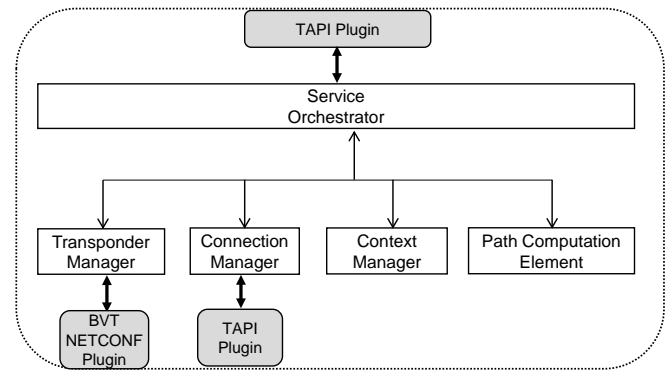


Fig. 4. Optical SDN controller architecture

workflow between the different modules. Also manages connectivity, topology and path computation services.

- Context topology manager: It composes the internal TAPI context topology and serves information from it. The internal TAPI context is composed of the context topology of the fronthaul OLS controller and their SIPs.
- Connection manager: It manages the TAPI connectivity service call and connections in the fronthaul OLS domain. The connection manager can support multiple plugins.
- The path computation element (PCE): It computes a path (nodes/links) between two SIPs based on certain traffic engineering metrics (e.g. unreserved bandwidth).
- Transponder manager: It is responsible for the management of the transponders. It can support multiple plugins, where each plugin is responsible for one type of transponder. We proposed a specific BVT NETCONF plugin. It is responsible of allocating the required optical bandwidth for the requested capacity, providing the initial configuration parameters of the OFDM-based BVT and processing the monitored per-subcarrier SNR to assign the optimal constellation in a closed-loop by using the Levin-Campello bit/power loading algorithm [26]. The transponder manager can support multiple plugins.

The SDN controller provides connectivity services between pairs of OFDM-based BVTs with autonomic reconfiguration of the per-subcarrier constellation based on the monitored SNR. Fig. 5 depicts an example of the workflow involved between the optical SDN controller and the BVT agents for the autonomic provisioning of connectivity services. The provisioning of a connectivity service request between two endpoints is sent to the service orchestrator by means of a TAPI POST HTTP request, specifying the two SIPs involved. This process triggers the following actions:

1) *Computation of required spectrum and path:* After the request is received by the service orchestrator, it requests to the transponder manager the required optical bandwidth (in GHz) from the requested capacity (in Gb/s). Specifically, the transponder manager computes the optical bandwidth from the requested capacity, which is aware of the transceiver supportable capabilities. It considers the worst-case scenario (i.e., without knowledge of the spatial path). Therefore, it computes the required optical bandwidth considering an uniform

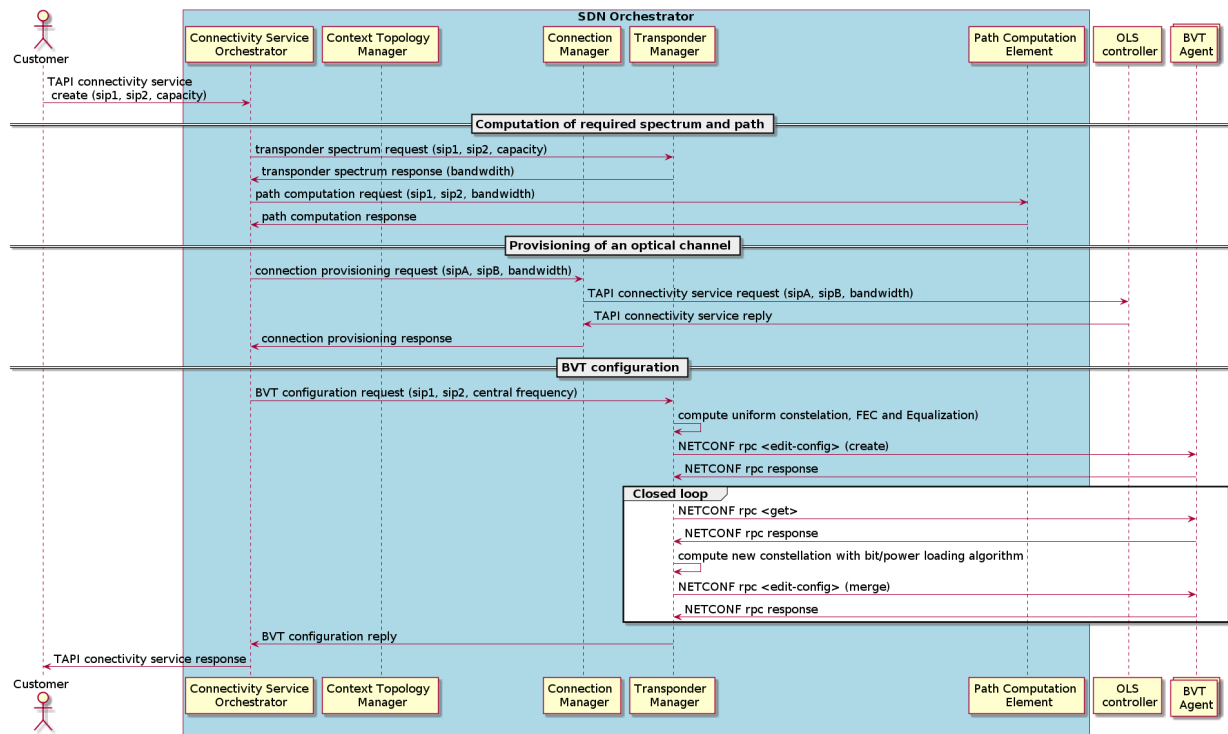


Fig. 5. Autonomic provisioning of a connectivity service with multi-adaptive BVTs.

constellation for all subcarriers with the lower number of bits per symbol, in order to meet the requested capacity. Then, the transponder manager replies with the computed optical bandwidth (e.g. 37.5 GHz) to the service orchestrator.

2) *Provisioning of the optical channel*: Next, the service orchestrator requests to the PCE the computation of an optical path between the two SIPs. If a feasible path is found, the service orchestrator requests to the connection manager the provisioning of an optical channel with the computed optical bandwidth. Then, the connection manager triggers a TAPI connectivity service call to the fronthaul OLS controller to provision a suitable connection. The OLS is responsible for the assignment of the frequency slot that meets the requested spectrum need.

3) *BVT configuration*: Once the connection is provisioned, the service orchestrator requests to the transponder manager the configuration of the involved BVTs. The transponder manager specifies the source and destination SIPs, and the nominal central frequency of the frequency slot assigned by the OLS. In order to do that, the transponder manager first allocates the constellation, the equalization and FEC between the source and destination BVTs. It considers again the worst-case scenario (i.e., without knowledge of the channel profile) and allocates an uniform constellation for all subcarriers with the lower number of bits per symbol. Next, the transponder manager configures the nominal central frequency, constellation, equalization and FEC in the BVT. It sends a NETCONF RPC <edit-config> (create) message to the BVT agent, and it notifies to the transponder manager if the configuration of the BVT was successful. This operation is performed both for the source BVT (transmitter (Tx)) and

the destination BVT (Receiver (Rx)).

4) *Closed loop*: Once both BVTs are configured successfully, the transponder manager starts a closed loop requests the SNR per sub-carrier at the BVT Rx by sending NETCONF RPC <get> messages to the BVT agent. Then, the transponder manager employs the Levin-Campello bit/power loading algorithm to compute the optimal constellation, including arbitrary sub-carrier suppression to adjust the spectrum of the signal. Finally, the transponder manager reconfigures the BVTs (Tx and Rx) as performed in the configuration phase, but sending NETCONF RPC <edit-config> (merge) messages to the BVT agents in order to update the constellation. Once the BVT are reconfigured with the new constellation, the transponder manager notifies to the service orchestrator. Next, the service orchestrator can notify with the TAPI that the connectivity service is provisioned. While the connectivity service is active, the transponder manager is working in a closed loop to continuously monitor the SNR per sub-carrier, apply the bit/power loading algorithm to recompute the constellation, and reconfigure the BVTs if required following the same steps as previously described. Finally, the transponder manager can delete the configuration from the source and destination BVTs by sending the NETCONF RPC <edit-config> (delete) messages to the BVT SDN agents when the service orchestrator get a connectivity service delete request.

IV. EXPERIMENTAL SETUP

The experimental setup used for validation is shown in Fig. 6, where a CO is providing connectivity to different RRUs using a passive optical network (PON) infrastructure featuring

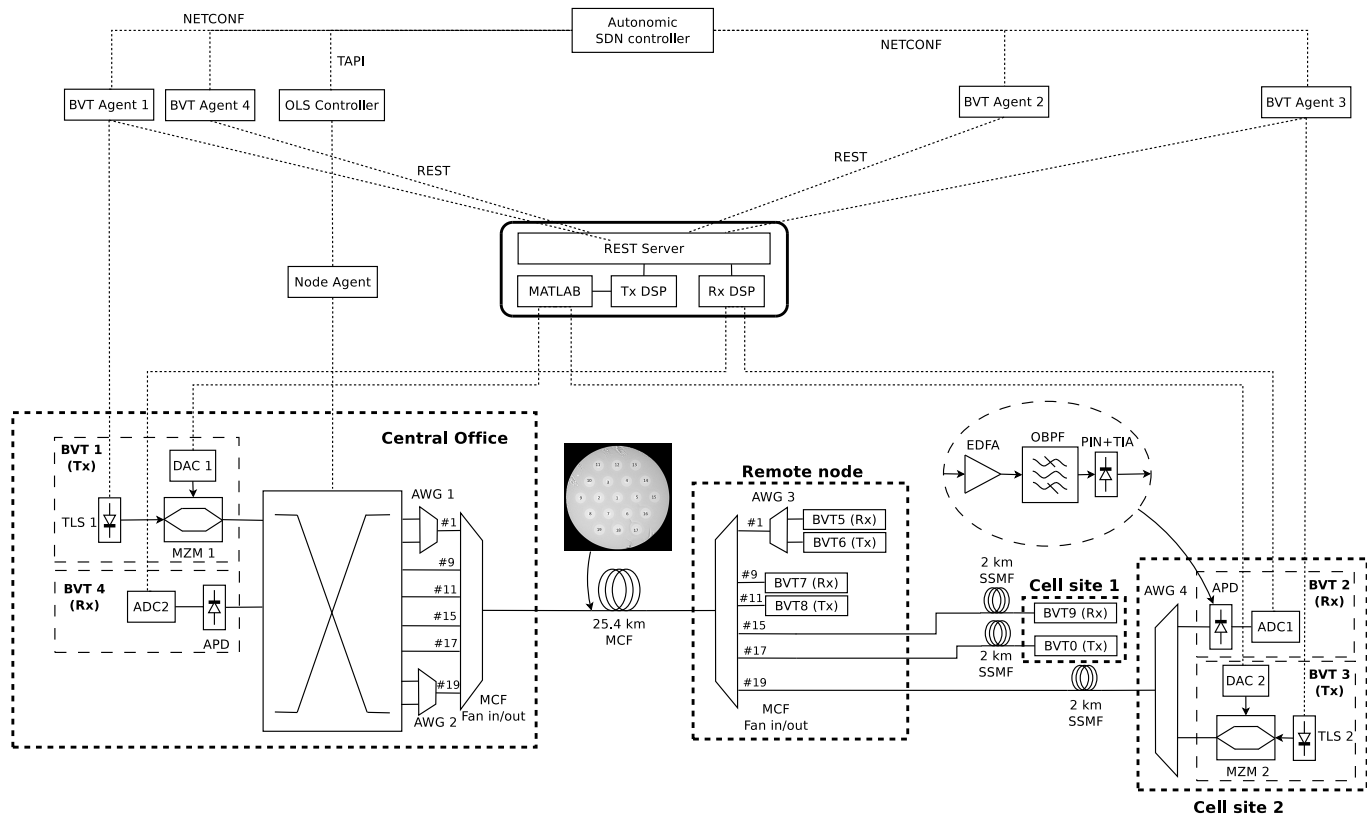


Fig. 6. Experimental setup.

TABLE II
BVT PARAMETERS.

BVT #	Nominal central frequency	Duplex
1	Tunable according the case	Adjustable
2	193.3 THz	WDM
3	193.2 THz	WDM
4	Tunable according the case	Adjustable
5	193.3 THz	WDM
6	193.2 THz	WDM
7	193.1 THz	SDM
8	193.1 THz	SDM
9	193.1 THz	SDM
0	193.1 THz	SDM

SDM and WDM. The CO is composed of a BVT pair, a 64×64 optical switching matrix and a 100-GHz AWG. The emulated PON infrastructure is composed by a 25.4-km 19-core MCF feeder segment, and a 2-km SSMF drop segment. In turn, the RN RRUs are composed of a 100-GHz AWG and a BVT pair. This is operated by means of the corresponding BVT agents, an OLS controller, a node agent and an SDN controller.

Since AWGs are used for achieving WDM, a rather fixed set of frequencies is used for the experiment, which are reported in Table IV. All the BVTs are configured to employ MMSE-based equalization.

The different BVTs are based on offline processing, hosted in an intermediate computer. Therefore Tx/Rx digital signal processing (DSP) is executed there according to the calls received by the different BVT agents through representational state transfer (REST) API. In this particular setup, the

BBUs and RRUs are implemented using off-line processing to handle the bit streams corresponding to 256 OFDM radio frames. Control and monitoring words are randomly generated. 22.25 Gb/s are transmitted, given the parameters mentioned in Section III, assuming $M = 10$ bits per sample and including the overheads due to fronthaul CPRI framing (7 %) and optical transmission (6.1 %). This is implemented in the programmable DSP Tx module using Python and Matlab software, which further processes the resulting digital samples to generate another digital OFDM signal (this one for the fronthaul transceiver) according to the constellation specified by the controller. A 4-channel high-speed digital to analog converter (DAC) (up to 64 GSa/s and 13 GHz electrical bandwidth) is used to convert the digital OFDM signals and provide electrical analog signals that are optically modulated using Mach-Zehnder modulators (MZMs). The MZMs are working at the quadrature point and modulate the light of the C-band tunable lightwave sources (TLSs) managed by the BVT agents.

Each receiver is based on direct detection. An avalanche photo-diode (APD) is emulated by the combination of a gain-stabilized erbium doped fiber amplifier (EDFA), an optical band pass filter and a PIN diode followed by the corresponding transimpedance amplifier. The receiver subsystem is calibrated to obtain -28 dBm sensitivity for a 10^{-3} BER using on-off keying transmission at 10.7 Gb/s. Please note that in case approaching a preamplified receiver with no APD emulation, performance can be further optimized. A real-time digital oscilloscope (up to 100 GSa/s and 20 GHz bandwidth) is used

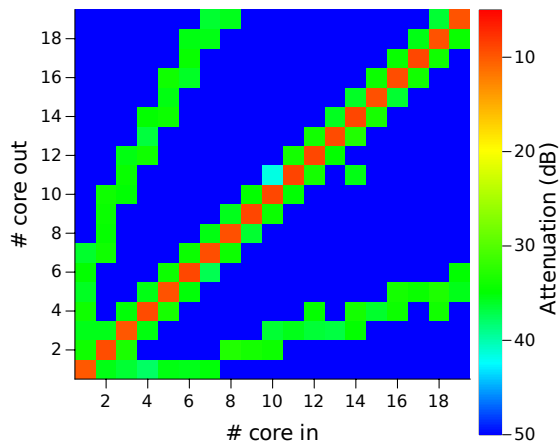


Fig. 7. MCF fiber loss/coupling characterization.

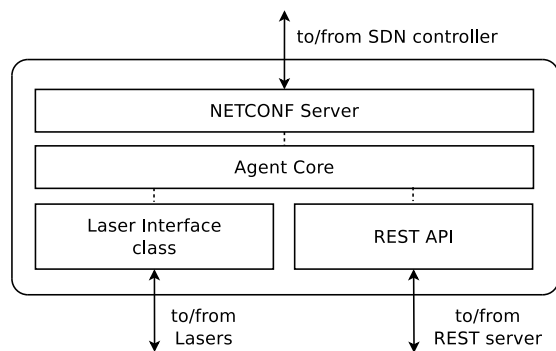


Fig. 8. BVT agent scheme.

as analog to digital converter (ADC). The digital signal is processed offline with the DSP Rx module based on Python to measure the per-subcarrier SNR and the overall BER.

The fiber network is implemented by using G.652D SSMF and a single feeder of a 25-km 19-core MCF. This feeder fiber has a diameter of 195 μm and a core to core distance of 34 μm . Cores have a diameter of 7.88 μm . A characterization of the fibre including fan-in/out devices is shown in Fig. 7. The average transmission loss is about 10 dB, while core to core crosstalk is below -23.7 dB. The latency introduced by the maximum fiber length is 123.3 μs .

The scheme of the implemented BVT agents to configure and monitor the BVTs is shown in Fig. 8. There, we can see that each agent is composed of a NETCONF server based on Python (pyang [32] and pyangbing [33]) that contains a modular YANG-based data store for the configuration and operational state data. The main element of the BVT agent is the agent core module that is responsible for mapping the high-level actions requested by the NETCONF server into several specific low-level actions on the involved optical sub-systems (i.e., laser and DSP Tx/DAC, and DSP Rx/ADC) by means of the developed function libraries and the corresponding interaction with the computer hosting the DSP modules.

A. Preliminary tests

The cases tested are summarized in Table IV-A. In order to assess their feasibility from the data plane perspective, a

TABLE III
CASES TESTED.

Case #	Description	BVTs involved
Case 1	CO-RN: WDM duplex	BVT1-BVT5 + BVT6-BVT4
Case 2	CO-RN: SDM duplex	BVT1-BVT7 + BVT8-BVT4
Case 3	CO-CS1: SDM duplex	BVT1-BVT9 + BVT0-BVT4
Case 4	CO-CS2: WDM duplex	BVT1-BVT2 + BVT3-BVT4

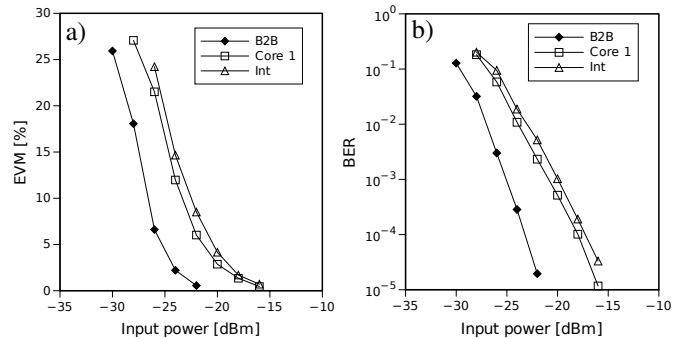


Fig. 9. Results of preliminary test for case 1. EVM (a) and BER (b) as function of the received power.

preliminary test is performed for case 1. Results are shown in Fig. 9 in terms of BER and EVM. First a back-to-back (B2B) configuration is evaluated and used as a reference. At -22 dBm, we obtain an EVM of 2.21 % ($2.85 \cdot 10^{-4}$ BER) after RRU processing while at -20 dBm the EVM is 0.6 % ($1.95 \cdot 10^{-5}$ BER) at the same point. Therefore, the 2.1 % EVM received power can be interpolated at -21.9 dBm. Next, the full case 1 (with fibre transmission) is evaluated. In fact, the received power for 2.1 % EVM can be estimated to be -19.0 dBm. Also, we introduce an interfering signal, similar to the one transmitted, over an adjacent core (#7) in order to evaluate crosstalk when measuring EVM and BER at core #1. To obtain the 2.1 % EVM under these circumstances, the received power is estimated to be -18.3 dBm, about 0.7 dB worse than in the previous case. Therefore, a 0.7 dB penalty per adjacent core should be taken into account when targeting SDM transmission over multiple cores in the same direction and wavelength.

V. EXPERIMENTAL RESULTS

We have experimentally validated the workflow depicted in Fig. 5, by following a set of the identifiable steps per each case (see Table IV-A cases) and the BVT connection pair (Tx and Rx):

- 1) Optical channel provisioning, corresponding to actions described in Sections III-B1 and III-B2.
- 2) Default configuration of the BVTs. This is related to actions detailed in Section III-B3.
- 3) Monitoring of the BVT Rx performance. At this point the control loop has been started as reported in Section III-B4.
- 4) Update of the configuration of the BVTs to optimize the performance. This is the actuator part of the action described in Section III-B4.
- 5) Delete of the optical channel.

No.	Time	Source	Destination	Protocol	Length	Info
17	0.064976507	SDN_CTRL	BVT1_AGENT	SSHv2	134	Client: Encrypted packet
118	34.483976829	SDN_CTRL	BVT1_AGENT	TCP	70	45372 → netconf-ssh(830)
134	34.624852091	SDN_CTRL	BVT2_AGENT	SSHv2	134	Client: Encrypted packet
293	249.941139324	SDN_CTRL	BVT2_AGENT	TCP	70	57136 → netconf-ssh(830)
319	250.188132150	SDN_CTRL	BVT1_AGENT	SSHv2	134	Client: Encrypted packet
410	274.472129157	SDN_CTRL	BVT1_AGENT	TCP	70	45376 → netconf-ssh(830)
427	274.778774181	SDN_CTRL	BVT2_AGENT	SSHv2	134	Client: Encrypted packet
547	360.611863332	SDN_CTRL	BVT2_AGENT	TCP	70	57140 → netconf-ssh(830)
563	443.549071588	SDN_CTRL	BVT3_AGENT	SSHv2	134	Client: Encrypted packet
666	477.675543516	SDN_CTRL	BVT3_AGENT	TCP	70	49490 → netconf-ssh(830)
680	478.027317244	SDN_CTRL	BVT4_AGENT	SSHv2	134	Client: Encrypted packet
789	687.28323597	SDN_CTRL	BVT4_AGENT	TCP	70	41956 → netconf-ssh(830)
802	687.635883212	SDN_CTRL	BVT3_AGENT	SSHv2	134	Client: Encrypted packet
907	712.325151216	SDN_CTRL	BVT3_AGENT	TCP	70	49494 → netconf-ssh(830)
923	712.615324380	SDN_CTRL	BVT4_AGENT	SSHv2	134	Client: Encrypted packet
1001	798.724533117	SDN_CTRL	BVT4_AGENT	TCP	70	41960 → netconf-ssh(830)
1018	818.078985530	SDN_CTRL	BVT2_AGENT	SSHv2	134	Client: Encrypted packet
1075	902.076978897	SDN_CTRL	BVT2_AGENT	TCP	70	57164 → netconf-ssh(830)
1092	1010.307751176	SDN_CTRL	BVT4_AGENT	SSHv2	134	Client: Encrypted packet
1131	996.235884710	SDN_CTRL	BVT4_AGENT	TCP	70	41968 → netconf-ssh(830)
1149	1004.133090227	SDN_CTRL	BVT1_AGENT	SSHv2	134	Client: Encrypted packet
1173	1009.293291528	SDN_CTRL	BVT1_AGENT	TCP	70	45414 → netconf-ssh(830)
1190	1009.360197623	SDN_CTRL	BVT2_AGENT	SSHv2	134	Client: Encrypted packet
1218	1010.529629648	SDN_CTRL	BVT2_AGENT	TCP	70	57178 → netconf-ssh(830)
1234	1014.471328158	SDN_CTRL	BVT3_AGENT	SSHv2	134	Client: Encrypted packet
1250	1019.585805612	BVT3_AGENT	SDN_CTRL	SSHv2	278	Server: Encrypted packet
1270	1019.683403412	SDN_CTRL	BVT4_AGENT	SSHv2	134	Client: Encrypted packet
1301	1020.740761812	SDN_CTRL	BVT4_AGENT	TCP	70	41992 → netconf-ssh(830)

Fig. 10. Wireshark screenshot for case 4 with relevant NETCONF messages between SDN controller and the BVT agents. Numbers represent the steps associated to each set of messages.

6) Delete of the BVTs.

This is repeated twice for each case, one time per each BVT pair. Furthermore, in order to test the performance of the BVT Rx monitoring operation, this is repeated one more time per BVT pair before deleting the optical channel and the BVTs.

Sample Wireshark screenshots are depicted in Figs. 10 and 11 for case 4. Fig. 10 shows the Wireshark screenshot with the beginning/end packages corresponding to the exchange of NETCONF messages between the SDN controller and the SDN agents. In turn, Fig. 11 depicts the Wireshark screenshot of the relevant messages between the OLS controller and node controller, and between the BVT agents and the intermediate computer hosting the DSP modules and interacting with the corresponding DACs and ADCs.

In the first step, the SDN controller configures the OLS controller, which sends the corresponding messages to the node controller in order to configure the switch matrix at the CO. This action corresponds to the messages framed as # 1 in Fig. 11. There we can observe the petition coming from the node controller and the reply message from the OLS controller.

In the second step, the SDN controller configures both BVT pairs to provision a bidirectional channel with a capacity of 22.25 Gb/s with the corresponding BVT parameters. In this initial step, regardless of the capacity demand, the same constellation is used for all the 512 subcarriers of the optical OFDM (bits per symbol = 2, and power per symbol = 1), in order to provide a fair channel estimation after step 3.

In the third step, the SDN controller requests to the BVT Rx agents the monitored SNR for the 512 subcarriers through the exchange of NETCONF messages as shown in Fig. 10. For each subcarrier, the DSP Rx performs the average of 10 ADC acquisitions of 20 μs in order to provide an accurate SNR. Please note that monitoring requests also return the BER measurement of the signals.

In Figs. 10-11 we can see the exchange of messages

No.	Time	Source	Destination	Protocol	Length	Info
2	0.006361	OLS_CTRL	NODE_CTRL	HTTP	224	POST /passion/sb1/opticalSwitch/connections HTTP/1.1 (application/json)
4	0.058429	NODE_CTRL	OLS_CTRL	HTTP	219	HTTP/1.0 200 OK (application/json)
8	9.974213	BVT1_AGENT	REST	HTTP	1298	POST /api/dac HTTP/1.1 (application/json)
10	31.716372	REST	BVT1_AGENT	HTTP	229	HTTP/1.0 200 OK (application/json)
14	34.157334	BVT2_AGENT	REST	HTTP	1325	POST /api/osc HTTP/1.1 (application/json)
24	140.6148	REST	BVT2_AGENT	HTTP	1075	HTTP/1.0 200 OK (application/json)
28	141.5927	BVT2_AGENT	REST	HTTP	1325	POST /api/osc HTTP/1.1 (application/json)
38	246.1751	REST	BVT2_AGENT	HTTP	1077	HTTP/1.0 200 OK (application/json)
46	249.7998	BVT1_AGENT	REST	HTTP	560	POST /api/dac HTTP/1.1 (application/json)
48	271.5446	REST	BVT1_AGENT	HTTP	229	HTTP/1.0 200 OK (application/json)
58	274.6301	BVT2_AGENT	REST	HTTP	587	POST /api/osc HTTP/1.1 (application/json)
65	357.4889	REST	BVT2_AGENT	HTTP	545	HTTP/1.0 200 OK (application/json)
67	443.4830	OLS_CTRL	NODE_CTRL	HTTP	224	POST /passion/sb1/opticalSwitch/connections HTTP/1.1 (application/json)
69	443.4499	NODE_CTRL	OLS_CTRL	HTTP	219	HTTP/1.0 200 OK (application/json)
73	453.2163	BVT3_AGENT	REST	HTTP	1298	POST /api/dac HTTP/1.1 (application/json)
75	474.9370	REST	BVT3_AGENT	HTTP	229	HTTP/1.0 200 OK (application/json)
79	477.5922	BVT4_AGENT	REST	HTTP	1325	POST /api/osc HTTP/1.1 (application/json)
89	586.9054	REST	BVT4_AGENT	HTTP	1163	HTTP/1.0 200 OK (application/json)
93	588.8806	BVT4_AGENT	REST	HTTP	1325	POST /api/osc HTTP/1.1 (application/json)
103	683.7151	REST	BVT4_AGENT	HTTP	1158	HTTP/1.0 200 OK (application/json)
107	687.2269	BVT3_AGENT	REST	HTTP	842	POST /api/dac HTTP/1.1 (application/json)
109	700.3324	REST	BVT3_AGENT	HTTP	229	HTTP/1.0 200 OK (application/json)
111	712.4331	BVT4_AGENT	REST	HTTP	123	POST /api/osc HTTP/1.1 (application/json)
113	795.4898	REST	BVT4_AGENT	HTTP	761	HTTP/1.0 200 OK (application/json)
117	816.7206	BVT2_AGENT	REST	HTTP	587	POST /api/osc HTTP/1.1 (application/json)
119	898.4047	REST	BVT2_AGENT	HTTP	585	HTTP/1.0 200 OK (application/json)
121	908.9522	BVT4_AGENT	REST	HTTP	123	POST /api/osc HTTP/1.1 (application/json)
123	992.6947	REST	BVT4_AGENT	HTTP	758	HTTP/1.0 200 OK (application/json)
126	1006.316	OLS_CTRL	NODE_CTRL	HTTP	145	DELETE /passion/sb1/opticalSwitch/connections HTTP/1.1 (application/json)
128	1006.368	NODE_CTRL	OLS_CTRL	HTTP	219	HTTP/1.0 200 OK (application/json)
130	1007.773	BVT1_AGENT	REST	HTTP	273	DELETE /api/dac/1 HTTP/1.1
132	1007.779	REST	BVT1_AGENT	HTTP	243	HTTP/1.0 200 OK (application/json)
134	1007.996	BVT2_AGENT	REST	HTTP	273	DELETE /api/osc/1 HTTP/1.1
136	1008.992	REST	BVT2_AGENT	HTTP	243	HTTP/1.0 200 OK (application/json)
138	1016.726	OLS_CTRL	NODE_CTRL	HTTP	145	DELETE /passion/sb1/opticalSwitch/connections HTTP/1.1 (application/json)
140	1016.766	NODE_CTRL	OLS_CTRL	HTTP	219	HTTP/1.0 200 OK (application/json)
142	1018.100	BVT3_AGENT	REST	HTTP	273	DELETE /api/dac/2 HTTP/1.1
144	1018.115	REST	BVT3_AGENT	HTTP	243	HTTP/1.0 200 OK (application/json)
146	1018.240	BVT4_AGENT	REST	HTTP	273	DELETE /api/osc/2 HTTP/1.1
148	1018.245	REST	BVT4_AGENT	HTTP	243	HTTP/1.0 200 OK (application/json)

Fig. 11. Wireshark screenshot for case 4. It shows the http messages exchanged between the OLS controller and the node agent; and between the BVT agents and the REST server that manages the hardware. Numbers represent the steps associated to each set of messages.

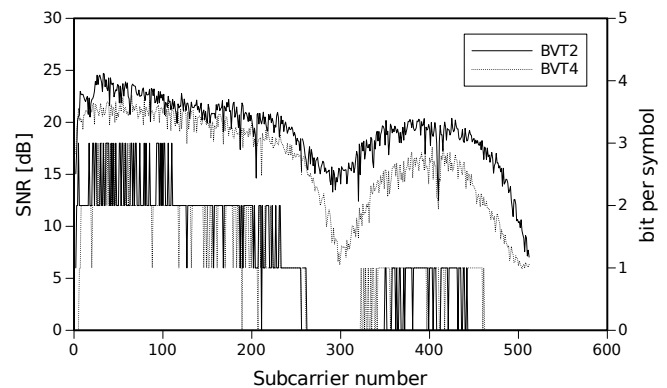


Fig. 12. Measured SNR and bit per symbol assignment for the BVTs examined.

between all the intervening entities to configure and test the performance of the different BVTs. In fact, in the 2+3 frame of Fig. 10, we can observe the messages for configuring and monitoring both BVTs pairs. Fig. 12 shows the monitored SNR and the new values of the constellation (bits per symbol) for each subcarrier. Significant changes are observed with respect to the initial uniform loading.

After reconfiguration, step 3 is launched again in order to crosscheck the performance. In Fig. 10 we can observe the messages exchanged between the controller and the agents of BVT2 and BVT4 in order to obtain the corresponding BER and SNR. These messages trigger the communication with the REST server, shown in Fig. 11 in order to perform the data acquisition at ADC and the suitable signal processing.

Finally, in the fifth and sixth steps, the SDN controller deletes the optical channel by first removing the connection of the switching matrix (step 5) and subsequently removing

TABLE IV
 AVERAGE CONFIGURATION TIME FOR ALL THE CASES TESTED.

	Time	Time exc. offline DSP
Step 1	60 ms	60 ms
Step 2+3	130 s	4 s
Step 3	90 s	4 s
Step 4	110 s	2 s
Step 5	1 s	1 s
Step 6	6 s	6 s

TABLE V
 BER OBTAINED FOR THE DIFFERENT CASES.

	Case 1	Case 2	Case 3	Case 4
CO, step 2	$3.7 \cdot 10^{-2}$	$4.4 \cdot 10^{-2}$	$5.9 \cdot 10^{-2}$	$4.3 \cdot 10^{-2}$
CO, step 4	$5.1 \cdot 10^{-5}$	$1.3 \cdot 10^{-5}$	$\leq 10^{-6}$	$3.9 \cdot 10^{-5}$
RN/CS, step 2	$7.4 \cdot 10^{-3}$	$9.6 \cdot 10^{-3}$	$1.1 \cdot 10^{-2}$	$9.2 \cdot 10^{-3}$
RN/CS, step 4	$7.5 \cdot 10^{-5}$	$\leq 10^{-6}$	$1.5 \cdot 10^{-5}$	$1.3 \cdot 10^{-5}$

the state in the BVTs (step 6). The messages for these actions are shown in Figs. 10-11. Precisely, Fig. 10 shows the message exchange between the SDN controller and the BVT agents, while Fig. 11 depicts the interaction between the BVT agents and the REST server, and also the messages between the node agent and the OLS controller.

Table IV summarizes the results in terms of configuration time. There we also include the time when excluding offline signal processing according to e.g. the results shown in Fig. 11. In fact, by subtracting these values to the time reported before, we can have an idea of the performance of the network in case the transceivers were working in real time. In this case, the configuration time of the different steps is 6 s or less for all the cases. Please note that steps 1, 5 and 6 do not involve offline DSP. The connection setup time is less than 5 s (excluding offline DSP), as it involves steps 1, 2 and 3. This value is well below the 90 min specified by the 5G infrastructure public private partnership [34]. Also, the results obtained are in the order of those found in [35], [36] (also excluding eventual offline DSP) which are based on Open-Config/OpenROADM interfaces. Please note that fronthaul is a service whose requirements are quite stable over time and network reconfiguration is not frequent. In fact, once the configuration is set, the control loop updates the configuration of the transceivers only in case a performance degradation is sensed when monitoring the BVTs.

Tables V and VI summarize the results in terms of BER and EVM, respectively. There we can see that when using the default configuration (after step 2), performance is quite bad and does not comply with the expected values. Nevertheless, after step 4, when bit/power loading is applied, BER is more

TABLE VI
 EVM OBTAINED FOR THE DIFFERENT CASES.

	Case 1	Case 2	Case 3	Case 4
CO, step 2	18.7 %	19.8 %	21.5 %	19.7 %
CO, step 4	0.9 %	0.5 %	0.1 %	0.8 %
RN/CS, step 2	10.1 %	11.2 %	11.3 %	11.0 %
RN/CS, step 4	1.0 %	0.1 %	0.5 %	0.5 %

than one order of magnitude below the $2.63 \cdot 10^{-4}$ limit obtained in Section III. In fact, as shown in Table VI, this leads to EVM values equal to 1 % and below, being suitable for the proposed radio signals with 256QAM constellation.

VI. CONCLUSION

We have experimentally demonstrated a passive network able to handle up to $19 \times 40 = 760$ spatial/spectral channels. In fact, a 256-QAM 760.32 MHz radio signal, featuring a total capacity of 5.667 Gb/s has been digitized to a 22.25 Gb/s DRoF data stream and successfully transmitted over this infrastructure. At the same time, we have shown how the capacity can be set by the SDN controller by generating the suitable constellation per OFDM subcarrier after monitoring the SNR, which gives an estimation of the channel profile. This allows to optimize the transmission performance according to the required capacity. In fact, we have shown that BER can be improved by about 3 orders of magnitude with respect to uniform loading, which leads to EVM figures of 1 % and below for the reconstructed radio signal.

This paves the way towards future fully automated networks, since the SDN controller assigns the right constellation per OFDM subcarrier at each transceiver, which can be advantageously combined with the knowledge of the network status, triggering the convenient actions.

ACKNOWLEDGMENT

The authors would like to thank Laura Rodríguez for her effort and help building up the hardware/software interfaces, and the anonymous reviewers whose comments and suggestions helped to improve the quality of this paper.

REFERENCES

- [1] A. Tzanakaki, M. Anastasopoulos, N. Gomes, P. Assimakopoulos, J. M. Fàbrega, M. S. Moreolo, L. Nadal, J. Gutiérrez, V. Sark, E. Grass *et al.*, "Transport Network Architecture," *5G System Design: Architectural and Functional Considerations and Long Term Research*, 2018.
- [2] 3GPP TS 38.211, "NR physical channels and modulation," Mar. 2019, 3GPP Rel. 15.
- [3] S. Rommel, D. Perez-Galacho, J. M. Fabrega, R. Muñoz, S. Sales, and I. Tafur Monroy, "High-Capacity 5G Fronthaul Networks Based on Optical Space Division Multiplexing," *IEEE Transactions on Broadcasting*, vol. 65, no. 2, pp. 434–443, June 2019.
- [4] J. M. Fabrega, R. Muñoz, M. S. Moreolo, L. Nadal, M. Eisel, F. Azen-dorf, J. P. Turkiewicz, P. W. L. van Dijk, S. Rommel, and I. T. Monroy, "Digitized Radio-over-Fiber Transceivers for SDM/WDM Back-/Front-Haul," in *2019 21st International Conference on Transparent Optical Networks (ICTON)*, July 2019, pp. 1–4.
- [5] L. Zhang, A. Udalcovs, R. Lin, O. Ozolins, X. Pang, L. Gan, R. Schatz, M. Tang, S. Fu, D. Liu, W. Tong, S. Popov, G. Jacobsen, W. Hu, S. Xiao, and J. Chen, "Toward Terabit Digital Radio over Fiber Systems: Architecture and Key Technologies," *IEEE Communications Magazine*, vol. 57, no. 4, pp. 131–137, April 2019.
- [6] J. M. Rivas-Moscoco, B. Shariati, A. Mastropaolo, D. Klonidis, and I. Tomkos, "Cost benefit quantification of sdm network implementations based on spatially integrated network elements," in *ECOC 2016; 42nd European Conference on Optical Communication*, Sep. 2016, pp. 1–3.
- [7] R. Munoz, N. Yoshikane, R. Vilalta, J. M. Fabrega, L. Rodriguez, D. Soma, S. Beppu, S. Sumita, R. Casellas, R. Martinez, T. Tsuritani, and I. Morita, "Adaptive software defined network control of space division multiplexing super-channels exploiting the spatial-mode dimension," *IEEE/OSA Journal of Optical Communications and Networking*, vol. 12, no. 1, pp. A58–A69, January 2020.

- [8] N. Sambo, P. Castoldi, A. D'Errico, E. Riccardi, A. Pagano, M. S. Moreolo, J. M. Fabrega, D. Rafique, A. Napoli, S. Frigerio, E. H. Salas, G. Zervas, M. Nolle, J. K. Fischer, A. Lord, and J. P. F. P. Giménez, "Next generation sliceable bandwidth variable transponders," *IEEE Commun. Mag.*, vol. 53, no. 2, pp. 163–171, Feb. 2015.
- [9] J. M. Fabrega, M. Svaluto Moreolo, L. Nadal Reixats, F. J. Vilchez, R. Casellas, R. Vilalta, R. Martínez, R. Muñoz, J. P. Fernández-Palacios, and L. M. Contreras, "Experimental validation of a converged metro architecture for transparent mobile front-/back-haul traffic delivery using SDN-enabled sliceable bitrate variable transceivers," *J. Lightw. Technol.*, vol. 36, no. 7, pp. 1429–1434, Apr. 2018.
- [10] M. Svaluto Moreolo, J. M. Fabrega, L. Nadal, F. J. Vilchez, A. Mayoral, R. Vilalta, R. M. noz, R. Casellas, R. Martínez, M. Nishihara, T. Tanaka, T. Takahara, J. C. Rasmussen, C. Kottke, M. Schlosser, R. Freund, F. Meng, S. Yan, G. Zervas, D. Simeonidou, Y. Yoshida, and K.-I. Kitayama, "SDN-enabled sliceable BVT based on multicarrier technology for multiflow rate/distance and grid adaptation," *J. Lightw. Technol.*, vol. 34, no. 6, pp. 1516–1522, Mar. 2016.
- [11] E. Riccardi, P. Gunning, O. G. de Dios, M. Quagliotti, V. López, and A. Lord, "An Operator view on the Introduction of White Boxes into Optical Networks," *J. Lightw. Technol.*, vol. 36, no. 15, pp. 3062–3072, Aug 2018.
- [12] M. A. Habibi, M. Nasimi, B. Han, and H. D. Schotten, "A comprehensive survey of RAN architectures toward 5G mobile communication system," *IEEE Access*, vol. 7, pp. 70 371–70 421, 2019.
- [13] S. Mikroulis, I. N. Cano, D. Hillerkuss *et al.*, "CPRI for 5G Cloud RAN? –Efficient Implementations Enabling Massive MIMO Deployment–Challenges and Perspectives," in *2018 European Conference on Optical Communication (ECOC)*. IEEE, 2018, pp. 1–3.
- [14] KyungWoon Lee, Jung Ho Park, and HyunDo Jung, "Comparison of digitized and analog radio-over-fiber systems over wdm-pon networks," in *2013 International Conference on ICT Convergence (ICTC)*, 2013, pp. 705–706.
- [15] J. K. Chaudhary, A. Kumar, J. Bartelt, and G. Fettweis, "C-RAN Employing xRAN Functional Split: Complexity Analysis for 5G NR Remote Radio Unit," in *2019 European Conference on Networks and Communications (EuCNC)*. IEEE, 2019, pp. 580–585.
- [16] O. Chabbouh, S. B. Rejeb, N. Agoulmine, and Z. Choukair, "Cloud RAN architecture model based upon flexible RAN functionalities split for 5G networks," in *2017 31st International Conference on Advanced Information Networking and Applications Workshops (WAINA)*. IEEE, 2017, pp. 184–188.
- [17] H. Wang, M. A. Hossain, and C. Cavdar, "Cloud RAN architectures with optical and mm-Wave transport technologies," in *2017 19th International Conference on Transparent Optical Networks (ICTON)*. IEEE, 2017, pp. 1–4.
- [18] F. Ponzini, K. Kondepu, F. Giannone, P. Castoldi, and L. Valcarenghi, "Optical access network solutions for 5G fronthaul," in *2018 20th International Conference on Transparent Optical Networks (ICTON)*. IEEE, 2018, pp. 1–5.
- [19] I. Chih-Lin, H. Li, J. Korhonen, J. Huang, and L. Han, "RAN revolution with NGFI (xHaul) for 5G," *J. Lightw. Technol.*, vol. 36, no. 2, pp. 541–550, 2017.
- [20] R. Muñoz, J. M. Fàbrega, R. Casellas, M. S. Moreolo, R. Vilalta, L. Nadal, and R. Martínez, "Elastic optical technologies and SDN/NFV control for 5G mobile x-haul," in *2017 IEEE Photonics Society Summer Topical Meeting Series (SUM)*, July 2017, pp. 9–10.
- [21] R. Muñoz, J. Fàbrega, R. Vilalta, M. S. Moreolo, R. Martínez, R. Casellas, N. Yoshikane, T. Tsuritani, and I. Morita, "SDN control and monitoring of SDM/WDM and packet transport networks for 5G fronthaul/backhaul," in *2018 IEEE Photonics Society Summer Topical Meeting Series (SUM)*. IEEE, 2018, pp. 151–152.
- [22] 3GPP TS 38.801, "Study on new radio access technology: Radio access architecture and interfaces," Mar. 2017, 3GPP Rel. 14.
- [23] R. Muñoz *et al.*, "Autonomic SDN Control of Multi-Adaptive OFDM-Based BVTs in Partially-Disaggregated SDM/WDM Fronthaul Networks," in *2019 European conference on optical communications (ECOC)*, Sept. 2019, pp. 1–4.
- [24] J. M. Fabrega, M. S. Moreolo, L. N. Reixats, F. J. Vilchez, R. Casellas, R. Vilalta, R. Martínez, R. M. noz, J. P. Fernández-Palacios, and L. M. Contreras, "Experimental validation of a converged metro architecture for transparent mobile front-/back-haul traffic delivery using sdn-enabled sliceable bitrate variable transceivers," *J. Lightwave Technol.*, vol. 36, no. 7, pp. 1429–1434, Apr 2018. [Online]. Available: <http://jlt.osa.org/abstract.cfm?URI=jlt-36-7-1429>
- [25] R. Muñoz, N. Yoshikane, R. Vilalta, J. M. Fàbrega, L. Rodríguez, R. Casellas, M. S. Moreolo, R. Martínez, L. Nadal, D. Soma, Y. Wakayama, S. Beppu, S. Sumita, T. Tsuritani, and I. Morita, "SDN Control of Sliceable Multidimensional (Spectral and Spatial) Transceivers with YANG/NETCONF," *J. Opt. Commun. Netw.*, vol. 11, no. 2, pp. A123–A133, Feb 2019. [Online]. Available: <http://jocn.osa.org/abstract.cfm?URI=jocn-11-2-A123>
- [26] L. Nadal, M. S. Moreolo, J. M. Fàbrega, A. Dochhan, H. Griebner, M. Eiselt, and J.-P. Elbers, "DMT modulation with adaptive loading for high bit rate transmission over directly detected optical channels," *J. Lightw. Technol.*, vol. 32, no. 21, pp. 3541–3551, Nov 2014.
- [27] CPRI, "Interface specification," Oct. 2015, v 7.0.
- [28] R. Muñoz, J. M. Fabrega, R. Vilalta, L. Rodríguez, L. Nadal, R. Casellas, and R. Martínez, "Autonomic sdn control of multi-adaptive ofdm-based bvts in fully-disaggregated sdm/wdm fronthaul networks," in *45th European Conference on Optical Communication (ECOC 2019)*. IET, 2019, pp. 1–4.
- [29] "CTTC ONS github repository for BVT yang model," 2019. [Online]. Available: <https://github.com/CTTC-ONS/BVT/tree/master/YANG>
- [30] R. Casellas, F. J. Vilchez, L. Rodríguez, R. Vilalta, J. M. Fàbrega, R. Martínez, L. Nadal, M. S. Moreolo, and R. Muñoz, "An ols controller for hybrid fixed/flexi grid disaggregated networks with open interfaces," in *2020 Optical Fiber Communications Conference and Exhibition (OFC)*. IEEE, 2020, pp. 1–3.
- [31] "ONF technical recommendation. Functional Requirements for Transport API," *ONF TR-527*, 2016.
- [32] "An extensible YANG validator and converter in Python," 2019. [Online]. Available: <https://github.com/mbj4668/pyang>
- [33] "A plugin for pyang that creates Python bindings for a YANG model," 2019. [Online]. Available: <https://github.com/robshakir/pyangbind>
- [34] The 5G Infrastructure Public Private Partnership, "5G Vision." [Online]. Available: <https://5g-ppp.eu/wp-content/uploads/2015/02/5G-Vision-Brochure-v1.pdf>
- [35] L. Nadal, M. Svaluto Moreolo, J. A. Hernández, J. M. Fabrega, R. Casellas, R. Muñoz, R. Vilalta, L. Rodríguez, F. J. Vilchez, and R. Martínez, "Sdn-enabled s-bvt for disaggregated networks: Design, implementation and cost analysis," *Journal of Lightwave Technology*, vol. 38, no. 11, pp. 3037–3043, 2020.
- [36] A. Scambelluri, A. Giorgetti, D. Scano, F. Cugini, and F. Paolucci, "Openconfig and openroadm automation of operational modes in disaggregated optical networks," *IEEE Access*, vol. 8, pp. 190 094–190 107, 2020.

Dr. Josep M. Fabrega (IEEE S'05 M'10 SM'17) received his PhD degree in signal theory and communications from UPC-BarcelonaTech, Barcelona, Spain, in 2010. Currently he is a Senior Researcher in the Optical Networks and Systems Department of CTTC, Castelldefels, Spain. He has participated or promoted over 30 R&D projects either funded by industry or the EU and Spanish national Research programmes. He is the author of 53 publications and coauthor of another 124 publications, including international journals, conferences and patent families; covering theoretical and practical aspects of transmission devices and systems for fiber optic communication networks.

Dr. Fabrega received the EuroFOS Best Student Research Award for his PhD thesis (2010) and he has been awarded by a PTA R&D Engineering Fellowship (2007) and the Torres Quevedo Fellowship (2011) by Spanish Ministry of Science and Technology. He serves as an elected member of board of stakeholders of Photonics21 European Technology Platform since 2018.

Dr. Raul Muñoz (IEEE SM'12) is graduated in Telecommunications Engineering and received a Ph.D. degree, both from the Universitat Politècnica de Catalunya (UPC), Spain. He is Head of the Optical Networks and Systems Department at CTTC. He has participated or promoted over 50 R&D projects funded by EC, Spanish Research programmes, and industrial contracts. He has been Project Coordinator of the FP7 EU-Japan STRAUSS project, and the H2020-MSCA-ITN ONFIRE project. He has served as general chair of ONDM 2020 & WWRF39, and TPC chair of ECOC 2015 & ONDM2019. He was elected academic member of the 5G IA Board, the Steering Board of WWRF and the Network2020 ETP (2015-2017). He has published over 85 JCR journal papers, 275 international conference papers, and 3 patents.

Dr. Laia Nadal (SM'18) obtained her MSc Telecommunication Engineering degree from UPC-BarcelonaTech university in July 2010. She obtained the European Master of Research on Information and communication Technologies (MERIT) from the Signal Theory and Communications (TSC) department of the UPC in 2012. She received her PhD degree from TSC department of the UPC in November 2014. In 2010, she was awarded with the FPI grant from the Spanish Ministry of Economy and Competitiveness (MINECO) to perform her PhD within the framework of the National project DORADO in the CTTC. From May to August 2013 she was a Visiting Ph.D. Scholar in ADVA Optical Networking (Germany). She currently is a Senior Researcher of the Communication Networks Division. Her research interests include signal processing and advanced modulation formats for optical communication systems.

Carlos Manso received the B.S. and M.S. degrees in Telecommunications Engineering from Universitat Politècnica de Catalunya (UPC) in Barcelona (Spain) in 2016 and 2018, respectively. He has been working in CTTC as a research assistant since 2018. Since 2020 he is also a PhD candidate focusing on cloud native transport networks orchestration and machine learning for SDN networks.

Dr. Michela Svaluto Moreolo (S'04-A'08-SM'13) received the M.Sc. degree in Electronics Engineering and the Ph.D. degree in Telecommunications Engineering from University Roma Tre, Rome, Italy, in 2003 and 2007, respectively. She currently is a Senior Researcher and the Coordinator of the Optical Transmission and Subsystems research line within the Optical Networks and Systems Department, at the Centre Tecnològic de Telecomunicacions de Catalunya (CTTC), Spain. She also serves as member of the CTTC Management Team, with the role of Director of Quality Programs. Her research interest areas include advanced programmable multi-dimensional transmission systems, software-defined multi-Tb/s photonic transceivers and photonic technologies for future optical networks. She has authored and co-authored more than 180 journal and international conference papers and two book chapters. She has organized different scientific events and serves as regular reviewer for high impact journals and as TPC member of various conferences in the field of optical communications and photonics (such as OFC, ECOC, Photonics West and OSA APC).

Dr. Ricard Vilalta (Girona, 1983) graduated in telecommunications engineering in 2007 and received a Ph.D. degree in telecommunications in 2013, both from the Universitat Politècnica de Catalunya (UPC). He joined CTTC in 2010, and he is a senior researcher in the Optical Networks and Systems Department. He is an active contributor in several standardization bodies such as ONF (OTCC), ETSI (NFV, ZSM), and IETF (CCAMP, TEAS). He is leading open source contributions and features in ETSI Open Source MANO (OSM). He has been involved in several international, EU, national and industrial research projects. Currently, he is Project Coordinator of 5GPPP TeraFlow project.

Dr. Ricardo Martínez (SM'14) received the M.Sc. and Ph.D. degrees, both in telecommunications engineering, from the UPC-BarcelonaTech University, Barcelona, Spain, in 2002 and 2007, respectively. He has been actively involved in several EU public-funded and industrial technology transfer projects. Since 2013, he is a Senior Researcher at CTTC in Castelldefels, Spain. His research interests include control and orchestration architectures for heterogeneous and integrated network, and cloud infrastructures along with advanced mechanisms for provisioning/recovering quality-enabled services.

Francisco Javier Vilchez (IEEE SM'20) graduated in Telecommunication Engineering by the Polytechnic University of Catalonia in April 2002, and also graduated in Electronics Engineering by the same school in March 2007. He joined the former CTTC Optical Networking Area (now Optical Networks and Systems Department) in February 2008, as Research Engineer (becoming Researcher in 2013). His work focuses mainly on hardware and firmware design and development for electronic and optical circuits. Furthermore, he is mainly involved on the continuous evolution of ADRENALINE tedtbed, by the implementation and integration of prototypes based on opto-electronic systems with the required interfaces for the management from the control plane. Since November 2010, he is Coordinator of the Optical Networks and Systems laboratory. He is IEEE Senior Member since August 2020.

Dr. Diego Pérez Galacho received the MSc in Telecommunication Engineering from Málaga University (Spain) in 2011. From 2011 until September 2013, he was working in the design of coherent receivers in III-V technology for the European project MIRTHE at the Photonics & RF research laboratory at Málaga University. In September 2013, he joined the Silicon Photonics research group at Paris-Sud University, where he worked on the development of silicon transceivers for the European projects PLAT4M and COSMICC. In October 2016, he defended my PhD entitled "High speed optical modulation, advanced modulation formats and mode division multiplexing in Silicon Photonics" at Paris-Sud University. Since October 2017 he works in the Photonics Research Labs at Polytechnic University of Valencia developing optical links with Spatial Division Multiplexing for fronthaul mobile networks in the European project BlueSpace. His research interests comprise devices based on periodic structures and analog and digital optical communication systems including polarization diversity and space division multiplexing.

Prof. Salvador Sales (S'93-M'98-SM'04) is Professor at the in the ITEAM Research Institute, Universitat Politècnica de València, Spain, since 2007. He received the M.Sc. and the Ph.D. degrees from the Universitat Politècnica de València (UPV). He was recognized with the Annual Award of the Spanish Telecommunication Engineering Association to the best Ph.D. on optical communications. He is co-author of more than 175 journal papers and 300 international conferences. He has been collaborating and leading some national and European research projects since 1997. His main research interests include optoelectronic signal processing for optronic and microwave systems, optical delay lines, fiber Bragg gratings, WDM and SCM lighthwave systems and semiconductor optical amplifiers.

Dr. Evangelos Grivas received his BSc in Physics from Aristotle University of Thessaloniki, Greece in 2002, and his MSc in Microelectronics from University of Athens, Greece in 2004. He was with the Institute of Microelectronics, NCSR "Demokritos", from 2004 to 2006. He was with the Optical Communications Laboratory, University of Athens, Greece, from 2005 to 2012, working for his PhD on Optical Communications, where he also served as a research associate on contract, leading the design and development of numerous demonstrators. He served as the head of R&D in Eulambia Advanced Technologies from 2013 to 2020. His current research interests include ARoF for 5G communications. He is currently with NanoMEGAS SPRL.

Dr. Jaroslaw P. Turkiewicz obtained his Ph.D. degree from Eindhoven University of Technology, The Netherlands in 2006 and D.Sc. degree from Warsaw University of Technology in 2014 in the area of optical communication. Over the years he developed many innovative optical transmission and switching solutions. He authored and co-authored of over 100 peer-reviewed scientific articles, e.g. in journals like Nature Photonics, IEEE Photonics Technology Letters and Optics Express as well as leading international conferences like ECOC, OFC and ICTON, including the ECOC and OFC post-deadline papers. He established and manages the most advanced in Poland and whole Central-East Europe, Photonic Communication Laboratory build in the framework of the Polish Innovative Economy Program (POIG) FOTEH project. He has been awarded, e.g. prestigious IEEE Photonics (LEOS) Graduate Student Fellowship, Warsaw University of Technology Rector Awards for educational and scientific achievements as well as Top Innovator at Telekomunikacja Polska. In 2019 he had been awarded by the Polish State with Cross of Merit for contribution to development of optical communication in Poland.

Dr. Simon Rommel (S'15 M'18) obtained his B.Sc. from University of Stuttgart, Germany in 2011 and in 2014 obtained M.Sc. degrees in Photonic Networks Engineering from Aston University, Birmingham, UK and Scuola Superiore Sant'Anna, Pisa, Italy. He completed his Ph.D. in 2017 at Technical University of Denmark, Kongens Lyngby, Denmark with research focused on photonic-wireless convergence and millimeter-wave radio-over-fiber, including a research stay at the National Institute of Information and Communications Technology, Koganei, Tokyo, Japan. Since 2017 he is with Eindhoven University of Technology, currently as assistant professor, continuing his work photonic and radio frequency technologies with a strong focus on implementations for 5G. He contributed to multiple national and European research projects, incl. H2020 blueSPACE as technical manager. Dr. Rommel is a member of IEEE, OSA, IET and VDE.

Prof. Idelfonso Tafur Monroy is Professor in Photonic Terahertz Systems at the department of Electrical Engineering of Eindhoven University of Technology since 2017 and since 2018 director of the Photonic Integration Technology Center (PITC). His research interests are in the area photonics technologies for Terahertz systems, converged electronic-photonic integrated circuits for applications in secure communications, sensing and computing. He is co-author of over 500 journal and conference papers and has graduated 22 PhD students. He is co-founder of the start-up Bifrost Communications on optical fiber access solutions.